



Published in final edited form as:

Cell Rep. 2020 April 21; 31(3): 107524. doi:10.1016/j.celrep.2020.107524.

Beta-Catenin Causes Adrenal Hyperplasia by Blocking Zonal Transdifferentiation

Emanuele Pignatti^{1,2,7}, Sining Leng^{1,3,7}, Yixing Yuchi^{1,2}, Kleiton S. Borges^{1,2}, Nick A. Guagliardo⁴, Manasvi S. Shah^{1,2}, Gerard Ruiz-Babot^{1,2}, Dulanjalee Kariyawasam^{1,2}, Makoto Mark Taketo⁵, Ji Miao^{1,2}, Paula Q. Barrett⁴, Diana L. Carlone^{1,2,6}, David T. Breault^{1,2,6,8,*}

¹Division of Endocrinology, Boston Children's Hospital, Boston, MA 02115, USA

²Department of Pediatrics, Harvard Medical School, Boston, MA 02115, USA

³Division of Medical Sciences, Harvard Medical School, Boston, MA 02115, USA

⁴Department of Pharmacology, University of Virginia, Charlottesville, VA 22947, USA

⁵Division of Experimental Therapeutics, Graduate School of Medicine, Kyoto University, Kyoto 606-8506, Japan

⁶Harvard Stem Cell Institute, Cambridge, MA 02138, USA

⁷These authors contributed equally

⁸Lead Contact

SUMMARY

Activating mutations in the canonical Wnt/ β -catenin pathway are key drivers of hyperplasia, the gateway for tumor development. In a wide range of tissues, this occurs primarily through enhanced effects on cellular proliferation. Whether additional mechanisms contribute to β -catenin-driven hyperplasia remains unknown. The adrenal cortex is an ideal system in which to explore this question, as it undergoes hyperplasia following somatic β -catenin gain-of-function (β cat-GOF) mutations. Targeting β cat-GOF to zona Glomerulosa (zG) cells leads to a progressive hyperplastic expansion in the absence of increased proliferation. Instead, we find that hyperplasia results from a functional block in the ability of zG cells to transdifferentiate into zona Fasciculata (zF) cells. Mechanistically, zG cells demonstrate an upregulation of Pde2a, an inhibitor of zF-specific cAMP/PKA signaling. Hyperplasia is further exacerbated by trophic factor stimulation leading to

This is an open access article under the CC BY-NC-ND license.

*Correspondence: david.breault@childrens.harvard.edu.

AUTHOR CONTRIBUTIONS

E.P., S.L., D.L.C., and D.T.B. conceptualized the study; E.P., S.L., and D.T.B. developed the methodology; E.P., S.L., Y.Y., M.S.S., G.R.-B., N.A.G., K.S.B., J.M., D.K., D.L.C., and D.T.B. designed experiments; E.P., S.L., and Y.Y. performed experiments; M.M.T. provided essential material and advice; E.P., S.L., D.L.C., and D.T.B. wrote the original manuscript with editorial inputs from all authors; D.L.C., P.Q.B., and D.T.B. provided supervision; and D.T.B. acquired funds.

SUPPLEMENTAL INFORMATION

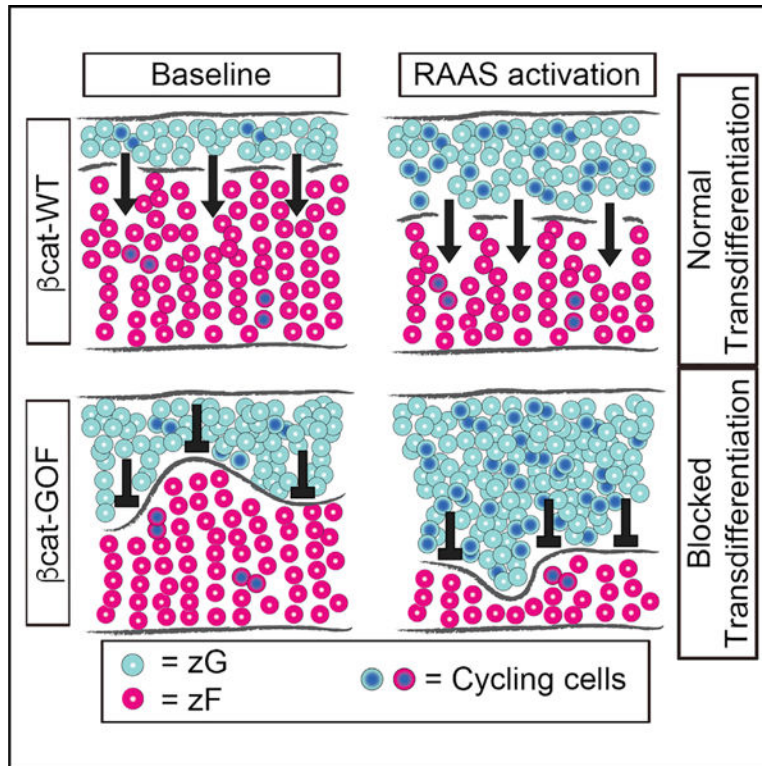
Supplemental Information can be found online at <https://doi.org/10.1016/j.celrep.2020.107524>.

DECLARATION OF INTERESTS

E.P., S.L., D.L.C., K.S.B., and D.T.B. declare provisional patent applications US19/38561 and US19/38564 related to this work.

organomegaly. Together, these data indicate that β -catenin drives adrenal hyperplasia through both proliferation-dependent and -independent mechanisms.

Graphical Abstract



In Brief

Using the adrenal cortex as a model for slow-cycling tissues, Pignatti et al. show that activation of the canonical Wnt/ β -catenin pathway leads to tissue hyperplasia by blocking cellular differentiation/cell-fate commitment, independent of its effects on cellular proliferation.

INTRODUCTION

The Wnt/ β -catenin signaling pathway is a key regulator of growth and development, driving both cellular proliferation and morphogenetic changes in a wide array of organisms (Goldstein et al., 2006; Huang and Niehrs, 2014; Kitajima et al., 2013; Loh et al., 2016; Schneider et al., 2015). This pathway also plays a critical role in mediating ongoing tissue maintenance in many organs, including the intestine, liver, brain, and adrenal cortex (Drelon et al., 2016; Nusse and Clevers, 2017; Vidal et al., 2016). Consistent with this role, constitutive activation of this pathway, either following somatic gain-of-function (GOF) mutations in β -catenin or loss-of-function (LOF) mutations in key negative regulators, such as APC (adenomatous polyposis coli) or in the transmembrane E3 ubiquitin ligase ZNRF3 (zinc and ring finger 3), leads to tissue hyperplasia and ultimately to neoplastic

transformation (Nusse and Clevers, 2017; Polakis, 2012). Whether the intrinsic proliferative capacity of a given tissue contributes to this hyperplastic response is unclear.

The adrenal cortex continuously turns over, renewing approximately every 1–3 months, despite having a relatively low proliferation rate (Chang et al., 2013; Zajicek et al., 1986). It is composed of distinct concentric zones that develop postnatally (Pignatti et al., 2017; Walczak and Hammer, 2015). The outermost layer, the zona Glomerulosa (zG) consists of aldosterone-producing cells, which give rise to the innermost layer, the glucocorticoid-producing zona Fasciculata (zF) through the process of zonal transdifferentiation and centripetal migration (Freedman et al., 2013; Pignatti et al., 2017). Recent studies have shown that high levels of Wnt/ β -catenin signaling within the zG contribute to the determination of zonal identity by both positively regulating the transcription of zG-specific genes (e.g., *Cyp11b2*, *Aldosterone Synthase*) and negatively regulating zF-specific genes (e.g., *Cyp11b1*, *11 β -hydroxylase*) (Basham et al., 2019; Berthon et al., 2010, 2014; Drelon et al., 2016; Heikkilä et al., 2002; Kim et al., 2008; Pignatti et al., 2017; Vidal et al., 2016; Walczak et al., 2014).

Constitutive activation of the Wnt/ β -catenin signaling pathway has been linked to adrenocortical hyperplasia and neoplastic transformation (Åkerström et al., 2016; Assié et al., 2014; Basham et al., 2019; Berthon et al., 2014; Tissier et al., 2005; Wang et al., 2017; Zheng et al., 2016). In fact, β -catenin GOF mutations and LOF mutations in APC and ZNRF3 are among the most common somatic changes in adrenocortical carcinoma (Assié et al., 2014; Lippert et al., 2018; Ragazzon et al., 2010; Tissier et al., 2005; Zheng et al., 2016). However, the cellular mechanisms responsible for adrenal hyperplasia following activation of this pathway remain unknown. To address this, we specifically targeted zG cells with a somatic β -catenin GOF mutation in mice. Our data reveal that the progressive hyperplastic expansion of the zG evoked by β cat-GOF results not from an increase in proliferation but rather from a block in zonal transdifferentiation that is exacerbated when combined with a proliferative stimulus. β cat-GOF adrenals also showed enhanced expression of *Pde2a* (*Phosphodiesterase 2A*), an inhibitor of the cAMP/PKA signaling pathway within the zF, suggesting that β cat-GOF may maintain zG identity in part through the suppression of zF identity. Together, our data identify a proliferation-independent mechanism, a block in zonal transdifferentiation, whereby β cat-GOF can cause tissue hyperplasia.

RESULTS

Stabilization of β -Catenin in zG Cells Results in Expansion of the zG

To investigate the cellular mechanisms by which activation of canonical Wnt/ β -catenin signaling leads to adrenal hyperplasia, we generated *AS^{Cre/+} :: Ctnnb1^{fllox(ex3)/+}* (β cat-GOF) mice by crossing mice harboring the zG-specific Aldosterone Synthase-Cre (*AS^{Cre/+}*) allele (Freedman et al., 2013) with mice harboring LoxP sites flanking the third exon of β -catenin (*Ctnnb1^{fllox(ex3)/+}*) (Harada et al., 1999) mice (Figure 1A). Deletion of the third exon of β -catenin results in an in-frame protein devoid of GSK3 β -specific phosphorylation sites that normally target β -catenin for degradation. Thus, in these mice β -catenin is stabilized specifically within zG cells and the β -catenin pathway is constitutively activated. For controls, we employed *AS^{Cre/+} :: Ctnnb1^{+/+}* mice (β cat-WT). Increased expression of *Axin2*

and *Lef1*, well-established β -catenin downstream targets, confirmed activation of this pathway in β cat-GOF adrenals (Figure 1B).

To begin to understand the impact of β cat-GOF on adrenal homeostasis over time, we analyzed the β -catenin expression domain in mice at different ages. β -catenin expression in β cat-WT adrenals was largely restricted to the zG at all ages (Figure 1C), consistent with a previous report (Basham et al., 2019). In contrast, β cat-GOF adrenals showed a progressive expansion of the region expressing β -catenin (β -catenin⁺) into the underlying zF region (Figure 1C; Figure S1A). Both sexes displayed a similar pattern in adult and aged mice (Figures S1B and S1C). Given that both male and female mice exhibited similar characteristics, unless otherwise noted, studies were performed with female mice.

To confirm that the expanded region arises from stabilized β -catenin⁺ cells, β cat-WT and β cat-GOF adrenals were co-stained with two β -catenin antibodies: one that recognizes total β -catenin and one that is specific to exon 3, the exon that is excised following recombination. In β cat-WT adrenals, we observed co-staining of cells underneath the capsule, corresponding to the morphological zG. Conversely, staining for β -catenin containing exon 3 was nearly completely absent from the expanded zG in β cat-GOF adrenals (Figure S1D). This result confirms that nearly all zG cells in the expanded region underwent recombination of the *Ctnnb1* locus. Additionally, to confirm active Wnt signaling within the expanded region, we co-stained for β -catenin and *Lef1*, which revealed that most β -catenin positive cells co-expressed *Lef1* (Figure S1E). For these and all subsequent studies, unless otherwise stated, the antibody that recognizes total β -catenin was used.

To confirm the cellular identity of β -catenin-expressing cells within the expanded region, we performed co-immunostaining for β -catenin and *Dab2*, an established zG marker (Romero et al., 2007). Similar to β cat-WT adrenals, *Dab2* expression co-localized with β -catenin in β cat-GOF adrenals (Figure 1D), indicating that cells within the expanded region maintained a zG-like identity. To further validate the zG identity of cells within the expanded β -catenin⁺ region, we performed immunostaining for $G\alpha_q$, the alpha subunit of the heterotrimeric G protein activated by Angiotensin II (AngII) in zG cells (Côté et al., 1997). Analysis of β cat-WT adrenals showed that $G\alpha_q$ co-localizes with both β -catenin and *Dab2* (Figure S1F). Consistent with their expression of *Dab2*, β -catenin⁺ cells in β cat-GOF adrenals also co-stained for $G\alpha_q$ (Figure 1E; Figure S1G). To rule out that these cells also exhibit zF-like features, we examined the expression pattern of aldo-keto reductase family 1 member B7 (*Akr1b7*), an established zF marker (Aigueperse et al., 1999), which revealed mutually exclusive expression of β -catenin and *Akr1b7* in both β cat-WT and β cat-GOF adrenals (Figure 1F).

To determine whether the expansion of the zG region resulted from hypertrophy or hyperplasia, we performed histomorphometric analysis of β cat-WT and β cat-GOF adrenals to assess changes in cell density. Analysis of the number of DAPI-positive nuclei per unit area (mm²) within each region revealed that the cellular density within the expanded zG region of β cat-GOF adrenals was indistinguishable from that within the zG region of β cat-WT adrenals (14,002 \pm 796 versus 13,704 \pm 780 nuclei/mm², respectively) and markedly different from the zF (6,838 \pm 502 versus 7,212 \pm 990 nuclei/mm², respectively) (Figure

1G), indicating that the expansion in the zG area in β cat-GOF mice is the result of hyperplasia and not hypertrophy. Consistent with a progressive hyperplastic increase in total mass of the zG-layer, overall adrenal weight was increased in aged β cat-GOF mice, compared with β cat-WT controls (Figure S1H). Together, these data show that stabilization of β -catenin within zG cells leads to a progressive hyperplastic expansion of the zG.

Stabilization of β -Catenin in zG Cells Blocks zG-to-zF Cell Transdifferentiation

To understand the cellular mechanisms underlying zG expansion in β cat-GOF mice, we first tested whether the hyperplastic expansion resulted from increased proliferation, a known response of elevated Wnt signaling (Nusse and Clevers, 2017). To address this, the proliferation index of zG cells in β cat-WT and β cat-GOF adrenals was determined by scoring the number of Ki67-positive cells per zG area. For these studies, β -catenin expression was used to define the zG. Although a modest increase in Ki67-positive cells was observed in the zG of β cat-GOF compared with control adrenals in both adult and aged mice (Figure S2A), when normalized by the zG area the fraction of proliferating cells was significantly decreased (Figure 2A). This result indicates that the expansion of β -catenin-expressing cells in β cat-GOF mice was likely not due to increased cell division. Since enhanced cell survival (i.e., reduced apoptosis) could also contribute to the expansion, we next assessed the impact of β cat-GOF on apoptosis by staining for activated caspase-3 or TUNEL in β cat-WT and β cat-GOF adrenals. No differences were observed between groups (Figures S2B–S2E), despite an overall low level of apoptosis. Thus, these results indicate that the zG expansion in β cat-GOF mice does not arise via changes in cell proliferation or cell death.

We next examined whether the expanded zG region in β cat-GOF adrenals resulted from a block in zonal transdifferentiation (Freedman et al., 2013). To address this, we performed functional lineage-tracing analysis using mTmG reporter mice (Muzumdar et al., 2007) (Figure 2B). Consistent with our prior findings (Freedman et al., 2013), GFP marked both zG cells (as defined by either Dab2 or G α q co-expression) and zF cells (defined by either Akr1b7 co-expression or the absence of Dab2 or G α q expression) in β cat-WT adrenals (Figures 2C–2E). In contrast, GFP expression in β cat-GOF adrenals was confined to zG cells, with nearly all zF cells negative for GFP expression (Figures 2C–2E) indicating a block in transdifferentiation. The few GFP-positive cells in the zF region failed to express β -catenin, establishing that these cells had escaped recombination of the *Ctnnb1*^{flox(ex3)} allele (Figure 2F, arrowheads). Together, these data indicate that stabilization of β -catenin within zG cells leads to progressive zG hyperplasia, in part, through a block in zonal transdifferentiation, defining a new paradigm for hyperplastic expansion.

β cat-GOF Leads to Induction of Pde2a, a Negative Regulator of the zF

Recently, phosphodiesterases were identified as potential negative regulators of zF identity. By hydrolyzing and inactivating cAMP, an essential signaling intermediate of the PKA signaling pathway, zF function is blocked (Mathieu et al., 2018) (Figure 3A). Phosphodiesterase activity within the adrenal gland is almost exclusively the result of PDE2A in the zG (MacFarland et al., 1991; Stephenson et al., 2009). To assess the impact of β cat-GOF on phosphodiesterase activity, we first performed quantitative real-time PCR for

Pde2a, which revealed a significant upregulation in β cat-GOF adrenals compared with controls (Figure 3B). In addition, immunohistochemical analysis detected *Pde2a* in the zG domain in control mice as well as the expanded zG domain in β cat-GOF adrenals overlapping with β -catenin expression (Figure 3D). We next performed immunostaining to assess the global phosphorylation status of downstream cAMP/PKA-substrates, which confirmed inhibition of cAMP/PKA signaling in the β -catenin-positive zG regions (Figure 3E).

To assess whether *Pde2a* is a direct target of canonical Wnt signaling, we searched for putative TCF/LEF consensus sequences (5'-A/T A/T CAAAG-3') within the promoter and first intron of the *Pde2a* gene locus. Chromatin immunoprecipitation (ChIP) analysis using anti- β -catenin antibody combined with whole adrenal extracts revealed two active TCF/LEF binding sites, located at positions +19,762 (first intron) and -8,545 (distal promoter) with respect to the transcriptional start site (Figure 3C). These two sequences were named Pde-A and Pde-B, respectively. A third putative TCF/LEF binding site, located at position +873 and named Pde-X, did not reveal β -catenin binding (Figure 3C). Altogether, these data suggest that β cat-GOF maintains a zG identity and blocks transdifferentiation, at least in part, through inhibition of zF identity by directly stimulating the expression of *Pde2a*, a key negative regulator of zF-dependent cAMP/PKA-mediated signaling.

Stabilization of β -Catenin in zG Cells Results in Mild Aldosteronism

Previous studies in mice and humans show a positive correlation between activation of Wnt signaling in the adrenal and increased steroidogenesis (Berthon et al., 2014; Teo et al., 2005; Wang et al., 2017; Wu et al., 2017). To determine whether stabilization of β -catenin within zG cells results in enhanced production of aldosterone, we quantified the plasma levels of aldosterone and plasma renin activity (PRA) in aged animals. β cat-GOF mice show an ~3.5-fold increase in the levels of aldosterone compared to β cat-WT mice (445 ± 317 pg/mL versus 131 ± 83 pg/mL, respectively) (Figure S3A). Despite this, analysis of PRA showed no difference between β cat-GOF and β cat-WT mice ($1,024 \pm 472$ ng/mL/h versus 716 ± 441 ng/mL/h, respectively) (Figure S3B). Thus, the increase in aldosterone production in β cat-GOF mice is insufficient to suppress the renin-AngII-aldosterone system (RAAS) and indicates that the relative decrease in zG-specific proliferation is not a consequence of altered RAAS activity.

Trophic Factor Stimulation Exacerbates the Block in Transdifferentiation

Feedback loops and tissue-specific trophic factors tightly regulate endocrine tissue mass. For example, chronic activation of RAAS has been associated with an increase in zG proliferation (McEwan et al., 1999; Nishimoto et al., 2014). To assess the impact of trophic factor induction on the β cat-GOF-induced block in transdifferentiation, we utilized *AS^{Cre/Cre}* mice (AS(KO)), a model of CYP11B2(AS) deficiency that results in a dramatic ~5-fold increase in RAAS activity from an early age (Freedman et al., 2013). By combining this model with the β cat-GOF model, we generated *AS^{Cre/Cre} :: Ctnnb1^{fllox(ex3)}* (AS(KO)- β cat-GOF) mice (Figures 4A and 4B). Activation of RAAS using AS(KO) mice led to an ~2-fold increase in the zG proliferative index in both β cat-WT and β cat-GOF mice, which was completely blocked by candesartan (an AngII receptor antagonist) (Figures 4C and 4D).

Next, we assessed the impact of enhanced trophic drive on zG area. Analysis of the zG (as defined by $G\alpha_q$ expression) revealed a notable expansion in AS(KO) mice compared with AS(Cre) controls ($54\% \pm 11\%$ of cortex in AS(KO) versus $16\% \pm 2\%$ in AS(Cre)) (Figures 4E and 4F). However, when combined with β -catenin stabilization (AS(KO)- β cat-GOF) the zG occupied nearly the entire cortex ($98\% \pm 4\%$) (Figures 4E and 4F). Remarkably, while a partial block in zG expansion was observed in AS(KO) controls ($24\% \pm 7\%$) following treatment with candesartan, it had no impact on zG area in AS(KO)- β cat-GOF mice ($98\% \pm 1\%$ of cortex) (Figures 4E and 4F). Moreover, gross analysis of adrenals from AS(KO)- β cat-GOF mice revealed a marked increase in weight (10.1 ± 5.5 mg) compared with adrenals from AS(KO), β cat-GOF, or β cat-WT mice (combined mean of 3.1 ± 0.8 mg), which was blocked by treatment with candesartan, AS(KO)- β cat-GOF (4.3 ± 2.2 mg) versus AS(KO) controls (2.6 ± 0.5 mg) (Figure 4G). Taken together, these results indicate that enhanced trophic drive via AngII induces zG expansion via cell proliferation, whereas β cat-GOF induces zG expansion via a block in transdifferentiation and that the combination of both leads to a dramatic increase in adrenal mass.

DISCUSSION

Wnt proteins are well-established growth stimulatory factors that drive cellular proliferation in a broad range of tissues (Nusse and Clevers, 2017). Aberrant activation of the Wnt/ β -catenin signaling pathway has also been implicated in the initiation and progression of numerous cancers, including adenocarcinoma of the colon and of the adrenal cortex (Nusse and Clevers, 2017; Polakis, 2012; Zhan et al., 2017). Given the diverse homeostatic mechanisms that regulate these tissues and their divergent rates of tissue turnover, it is possible that activation of Wnt/ β -catenin signaling may have multiple distinct downstream effects. In the intestine, a rapidly cycling tissue, stabilization of oncogenic β -catenin or deletion of key tumor-suppressor genes results in a prompt increase in proliferation leading to tissue hyperplasia (Barker et al., 2009; Koo et al., 2012; Romagnolo et al., 1999; Sansom et al., 2007). In contrast, how activation of Wnt/ β -catenin signaling drives hyperplasia in the adrenal cortex, a slowly cycling tissue, is not well understood. Our data show that β cat-GOF mice develop zG hyperplasia via a block in zonal transdifferentiation rather than an increase in cell proliferation (Figure 4H). In addition, we found no change in PRA between β cat-GOF and β cat-WT mice indicating that suppression of RAAS activity does not play a significant role in modulating the zG response to β cat-GOF. In contrast, activation of RAAS leads to exacerbation of the block in transdifferentiation and can lead to frank adrenomegaly, an observation with potential clinical consequence. Altogether, our data raise the intriguing possibility that activation of Wnt/ β -catenin signaling may contribute to hyperplastic expansion in a range of tissues through effects on cellular differentiation/cell-fate commitment, independent of proliferation, especially in neoplasms arising in slowly cycling tissues (e.g., adrenocortical carcinoma, medulloblastoma, craniopharyngioma, and thyroid carcinoma) (DeSouza et al., 2014; Sastre-Perona and Santisteban, 2012; Sekine et al., 2002).

Several recent studies have assessed proliferation in the adrenal cortex following activation of Wnt/ β -catenin signaling. Sporadic activation of β cat-GOF within the adrenal cortex, using an *Akr1b7* minimal promoter Cre driver that targets a subset of both zG and zF cells, leads to ectopic zG expansion in 5-month-old mice without an increase in proliferation

(Berthon et al., 2010, 2014). More recent analysis of ZNRF3 LOF within the adrenal cortex, using a steroidogenic factor 1 (Sf1-Cre) driver that targets all zG and zF cells, revealed adrenal hyperplasia and a corresponding increase in zF proliferation (Basham et al., 2019). In contrast, the zG cells in the Sf1-Cre model did not show an increase in proliferation (Basham et al., 2019), consistent with the overall decrease in proliferation in our model following β cat-GOF. Also, in contrast to our β cat-GOF model, activation of Wnt/ β -catenin signaling in zG cells, following ZNRF3 LOF, was not sufficient to block transdifferentiation of zG to zF cells (Basham et al., 2019), consistent with a reduced dose effect of ZNRF3 LOF on canonical Wnt/ β -catenin compared with our β cat-GOF model.

Adrenal physiology and the incidence of adrenal disease are influenced by sex differences, in both humans and mice (Crona and Beuschlein, 2019; El Wakil et al., 2013). Female mice have larger adrenals and show higher circulating levels of aldosterone and corticosterone compared with males (Bielohuby et al., 2007; Spinedi et al., 1992). A recent study designed to elucidate cellular and molecular mechanisms underlying these sexually dimorphic traits led to the discovery that female mice utilize a progenitor/stem cell compartment located in the capsule, which is actively suppressed by male hormones (Grabek et al., 2019). In contrast, adrenocortical homeostasis in male mice relies on proliferation within steroidogenic cells themselves (Grabek et al., 2019). In addition, male hormones have been shown to increase canonical WNT signaling within the adrenal, which serves to antagonize PKA signaling leading to slower adrenocortical turnover (Dumontet et al., 2018). To investigate the impact of sex on the β cat-GOF-induced block in transdifferentiation, we studied male and female mice at both adult and aged time points. The results of this analysis revealed no differences in the pattern of zG cell accumulation between male and female β cat-GOF mice, indicating that sex is not an important determinant of this trait.

Recently, the maintenance of two adjacent, functionally distinct, zones such as the zG and the zF, has been ascribed to the reciprocal inhibitory effects of the cAMP/PKA and the Wnt/ β -catenin pathways, in the zF and the zG, respectively (Drelon et al., 2016; Mathieu et al., 2018; Walczak et al., 2014). Phosphodiesterases have emerged as potential inhibitors of zF identity, as their expression is physiologically suppressed in the zF by the epigenetic regulator EZH2 (Mathieu et al., 2018). zG-specific expression of PDE2A is highly conserved among several species, including mice and humans (Stephenson et al., 2009), suggesting that PDE2A exerts a conserved function in the zG. Despite this, little is known regarding its role in adrenal zonation. Our data indicate that PDE2A is a direct target of Wnt/ β -catenin signaling and may function, at least in part, as an inhibitor of zF identity by suppressing cAMP/PKA signaling. This hypothesis is consistent with a previous study indicating that PDE2A is over-expressed preferentially in adrenal tumors carrying activating mutations in the gene encoding β -catenin (Durand et al., 2011). Altogether, our results encourage further studies on the potential role of phosphodiesterases in regulating zonation and potentially transdifferentiation within the adrenal cortex.

We previously showed that an ongoing process of zG-to-zF zonal transdifferentiation during postnatal development is the main source of zF cells (Freedman et al., 2013), though the mechanisms that regulate this process remain poorly understood (Pignatti et al., 2017). Under conditions where transdifferentiation is absent, the zF can be maintained by

alternative cellular pathways (Freedman et al., 2013). Whether similar alternative pathways are responsible for zF maintenance in the β cat-GOF mice remains to be determined. An alternative cellular pathway for maintenance of the zF might involve recruitment of subcapsular and/or capsular progenitor cells, which bypass the zG state. Another possibility might involve replication of zF cells formed during fetal development, prior to the development of the zG during early post-natal life. Testing such models will be important avenues for future research.

Chronic activation of RAAS has been implicated in cardiovascular end-organ damage independent of its role in regulation of intravascular volume and blood pressure (Crowley et al., 2006; Muñoz-Durango et al., 2016). Like other endocrine tissues, the zG is regulated by a feedback loop that involves AngII, an essential trophic factor that controls zG cell proliferation (McEwan et al., 1999; Nishimoto et al., 2014). Consistent with this, we found that chronic activation of RAAS in the setting of aldosterone synthase deficiency leads to an increase in cellular proliferation in both β cat-GOF mice and β cat-WT mice. These findings suggest that RAAS activation, and specifically AngII, may contribute to GOF events with potentially important clinical implications in the context of somatic and/or germline mutations that lead to β cat-GOF within the zG. Delineation of the impact of chronic RAAS activation will require careful retrospective analysis in patients discovered to have underlying β cat-GOF mutations at the time of resection or prospective analysis in cohorts with germline mutations.

In conclusion, our work provides new mechanistic insight into the control of adrenocortical zonation, by demonstrating that the Wnt/ β -catenin pathway drives zG hyperplasia by blocking zonal transdifferentiation, potentially through augmentation of negative regulators of the cAMP/PKA signaling pathway and zF identity. Further, our finding that RAAS activation is an important enhancer of β cat-GOF-induced hyperplastic zG expansion may have important clinical implications for the treatment of patients with somatic or germline mutations leading to activation of Wnt/ β -catenin signaling within the adrenal cortex.

STAR★METHODS

LEAD CONTACT AND MATERIALS AVAILABILITY

Further information and requests for resources and reagents should be directed to and will be fulfilled by the Lead Contact, David T. Breault (david.breault@childrens.harvard.edu). This study did not generate new unique reagents.

EXPERIMENTAL MODEL AND SUBJECT DETAILS

All animal procedures were approved by the Boston Children's Hospital Institutional Animal Care and Use Committee. Generation of the aldosterone synthase (AS)-Cre strain ($Cyp11b2^{tm1.1(cre)Brlt}$) was previously described (Freedman et al., 2013). To generate bigenic $Cyp11b2^{tm1.1(cre)Brlt/+}; Ctnnb1^{tm1Mmt}$ mice (referred to as β cat-GOF or bGOF), the $Cyp11b2^{tm1.1(cre)Brlt}$ strain was crossed with the $Ctnnb1^{tm1Mmt}$ strain (Harada et al., 1999). To generate trigenic $Cyp11b2^{tm1.1(cre)Brlt/+}; Ctnnb1^{tm1Mmt}; Gt(ROSA)26Sor^{tm4(ACTB-tdTomato,-EGFP)Lu0/J}$ mice (referred to as β cat-GOF::mTmG), the

β cat-GOF mice were crossed with the *Gt(ROSA)26Sor^{tm4}(ACTB-tdTomato,-EGFP)Luo/J* (mTmG) Cre-reporter line (Muzumdar et al., 2007). AS deficiency was achieved by breeding the AS-Cre allele to homozygosity (AS(KO) mice), as previously described (Freedman et al., 2013). AS(KO)- β cat-GOF mice were bred by intercrossing AS(KO) mice with *Ctnnb1^{tm1Mmt}* mice. All mice were maintained on a mixed sv129-C57BL/6 genetic background, with free access to food and water, under a 12-hour light/12-hour dark cycle. Mice were housed in a specific-pathogen-free grade facility, in an OptiMICE cage system, in groups of 2 to 5 animals per cage. All mice used for the experiments were drug and test naive. Female mice were used unless otherwise stated. To control for genetic background, whenever possible, experiments were performed using littermate control mice (β cat-WT or bWT) that did not carry the *Ctnnb1^{tm1Mmt}* allele and were positive for the *Cyp11b2^{tm1.1(cre)Brlt}* and the *Gt(ROSA)26Sor^{tm4}(ACTB-tdTomato,-EGFP)Luo/J* allele. Throughout the main text, mice heterozygous for the AS-Cre allele are referred to as *AS^{Cre/+}*, and mice heterozygous for the *Ctnnb1^{tm1Mmt}* allele are referred to as *Ctnnb1^{flox(ex3)/+}*. Studies were conducted on age-matched cohorts of mice that were ‘young adult’ (10 weeks of age), ‘adult’ (15-to-21 weeks of age) or ‘aged’ (38-to-53 weeks of age).

METHOD DETAILS

Gene Expression Analysis—RNA was purified from whole adrenals cleaned of adherent fat and homogenized in TRI® Reagent (Sigma) using the Direct-zol™ RNA kit (Zymo Research), following the manufacturer’s protocol. Further processing of total RNA involved reverse transcription into cDNA using the High-Capacity cDNA Reverse Transcription Kit (Life Technologies). Gene expression analysis was performed by Real Time quantitative PCR (RTqPCR) using the QuantStudio 6 Flex thermocycler (Life Technologies). Technical duplicates were used to control for technical variability. The TaqMan Universal PCR Master Mix and the following Taqman primers from Life Technologies were used: *Axin2* (Mm00443610_m1), *Lef1* (Mm00550265_m1), *Cyp11b2* (Mm01204955_g1), *Pde2a* (Mm01136644_m1) and *Actb* (Mm026119580_g1). *Actb* transcripts, encoding β -actin, were used as the internal control and data were expressed using the $2^{-\text{ddCt}}$ method. Sample size was estimated based on the published literature and our experience and is indicated in the figure legends.

Tissue preparation, immunofluorescence, microscopy and quantification—Mouse adrenals were cleared of adherent fat, weighed, fixed in 4% paraformaldehyde for 1 to 3 hours at 4°C, dehydrated in ethanol, xylene and embedded in paraffin blocks. Five μm -thick sections were processed for immunostaining by stepwise rehydration and permeabilization with 50 mM Tween-20 in PBS. Antigen retrieval was performed in 10 mM Sodium Citrate pH 6.0. Blocking was performed with 0.3% Tween-20 (Merck Millipore), 0.5% bovine serum albumin (BSA, Sigma), 10% normal goat serum (Sigma) in PBS, for 1h at room temperature. 0.5% sodium dodecyl sulfate (SDS, Fisher BioReagents) was also added to the blocking solution specifically when the primary anti-AS antibody was used (see below for antibody details). Immunostaining was done using the following primary antibodies: anti- β -catenin (mouse monoclonal, BD Biosciences, 610153; and rabbit polyclonal, Abcam, ab16051), anti-GFP (chicken polyclonal, Aves Labs, GFP-1020), anti-activated Caspase 3 (rabbit monoclonal, BD Biosciences, 559565), anti-Dab2 (mouse

monoclonal, BD Biosciences, 610464), anti-Akr1b7 (rabbit polyclonal, kindly provided by Dr. Pierre Val and Dr. Antoine Martinez (Aigueperse et al., 1999; Berthon et al., 2010)), anti-Gαq (rabbit polyclonal, Abcam, ab75825), anti-AS (rabbit polyclonal, kindly provided by Dr. Celso E. Gomez-Sanchez (Freedman et al., 2013)), anti-Ki67 (rabbit monoclonal, Lab Vision, RM-9106), anti-Lef1 (rabbit monoclonal, Abcam, ab137872), anti-Phospho-(Ser/Thr) PKA Substrate Antibody (rabbit polyclonal, Cell Signaling Technology, 9621), anti-β-catenin(ex3) (rabbit monoclonal, Abcam, ab32572), anti-PDE2A (rabbit polyclonal, Proteintech, 55306–1-AP). TUNEL staining was performed using the Click-iT™ Plus TUNEL Assay (Invitrogen), according to manufacturer's instructions. All primary antibodies were used at a 1:200 dilution and secondary antibodies at a 1:500 dilution. We used the following secondary antibodies for indirect staining: donkey anti-rabbit conjugated with Alexa Fluor 647, goat anti-mouse Alexa Fluor 594 and goat anti-chicken Alexa Fluor 488 (Molecular Probes). Sections were counter-stained with DAPI (4',6-diamidino-2-phenylindole) and mounted in Prolong Gold Mount Solution (Thermo Fisher Scientific). Images were captured with a Nikon upright Eclipse 90i microscope. For every image, three Z stacks were collected and deconvoluted to obtain the best resolution using the LIS-Elements Nikon software. Background autofluorescence was acquired from an empty green or red channel to allow subsequent subtraction of autofluorescence (e.g., from red blood cells and lipofuscin) from the other channels using the Image Calculator tool in Fiji software (Schindelin et al., 2012) (open source). Quantification of AS-, Ki67-, TUNEL- and activated Caspase 3-positive cells or Gαq and β-catenin-positive areas was performed using one complete equatorial section per mouse adrenal. Absolute cell numbers were normalized by zone-specific area (mm²), as indicated. Quantification of nuclear density was performed on representative regions of interest from equatorial sections by counting DAPI-positive nuclei per zone-specific area (mm²). Multiple measurements were taken from different regions of zG on βcat-GOF sections, to better address the complexity of the tissue. At least three replicates were performed for each experiment. Each replicate was generated from tissue from different mice.

Hormone Analysis—Plasma was collected in a stress-free environment by rapid non-terminal retro-orbital blood draw using thin hematocrit capillaries (Fisher Scientific). Aldosterone levels were determined on heparinized plasma (pre-diluted 2.5 times in PBS + 0.1% BSA) using an aldosterone I125 radioimmunoassay according to the manufacturer's instructions (Tecan). Plasma renin activity was determined on EDTA-collected plasma using a competitive radioimmunoassay for Angiotensin I following the manufacturer's instructions (Tecan). To rule out the impact of limiting amounts of angiotensinogen substrate in the plasma, an excess (about 180 ng) of angiotensinogen 1–14 renin substrate porcine (Sigma) was added to every sample, calibrator and control before quantification.

Chromatin immunoprecipitation (ChIP) assay—ChIP was performed using the High-Sensitivity ChIP Kit (Abcam, ab185913) following the manufacturer's instructions with minor modifications. Adrenals from C57BL/6J mice were collected, cleaned of adherent fat, weighed, snap frozen in liquid nitrogen and stored at –80 °C. Twelve adrenals (20 mg of tissue) were combined and briefly homogenized with a bench-top TissueLyser II (QIAGEN), followed by crosslinking using 1% formaldehyde for 15 min at room temperature. This

reaction was quenched with 1.25 M glycine. Samples were washed with ice cold PBS and homogenized in Lysis Buffer containing Protease Inhibitor Cocktail (from the High-Sensitivity ChIP Kit). After washing, chromatin was sheared into 100–300 bp fragments using a Probe Sonicator (Misonix Inc.) and the concentration of chromatin DNA was determined using NanoDrop (Thermo Fisher Scientific). To perform the immunoprecipitation (IP) assay 0.8 µg of antibody was combined with 2 µg of chromatin DNA, using each of the following antibodies: anti-β-catenin (Cell Signaling, 9581s), anti-Histone H3 (Abcam, ab1791) as positive control, and Non-Immune IgG (from the High-Sensitivity ChIP Kit) as negative control. Immuno-complexes and small aliquots of lysate (for input controls) were subjected to reverse crosslinking, release and purification of DNA using DNA Release Buffer and RNase A (from the High-Sensitivity ChIP Kit). Quantification of DNA levels was performed by RTqPCR analysis using Power SYBR® Green PCR Master Mix (4367659, Thermo Fisher Scientific) in a QuantStudio 6 Flex thermocycler (Life Technologies). Primers are listed in Table S1.

QUANTIFICATION AND STATISTICAL ANALYSIS

Two-tailed Student's *t*-Test was used for comparisons between groups of two. For every comparison, the F-test was used to assess whether two groups had different variances. If this was the case, the two-tailed Welch *t* test was used instead of the Student's *t*-Test. One-Way or Two-Way ANOVA and Tukey post hoc analysis (multiple comparison test) were used for comparisons between groups of three or more, unless otherwise specified. Prism 7 software (GraphPad) was used for statistical analysis. No power analysis was performed, size estimation was based on published literature and on our experience. All data were included, no exclusion method was applied. The statistical details of the experiments can be found in the figure legends, whereby 'n' values correspond to the number of independent mice. Data are presented as Mean ± Standard Error of the Mean (SEM).

DATA AND CODE AVAILABILITY

This study did not generate/analyze datasets/code.

Supplementary Material

Refer to Web version on PubMed Central for supplementary material.

ACKNOWLEDGMENTS

We thank members of the Breault Lab and Joseph A. Majzoub for helpful discussion and comments on the manuscript. We thank the BIDMC Histology Core for providing excellent technical expertise. This work was supported by R01-DK100653 and R01-DK119488A (D.T.B.).

REFERENCES

Aigueperse C, Martinez A, Lefrançois-Martinez AM, Veyssi re G, and Jean CI (1999). Cyclic AMP regulates expression of the gene coding for a mouse vas deferens protein related to the aldo-keto reductase superfamily in human and murine adrenocortical cells. *J. Endocrinol* 160, 147–154. [PubMed: 9854186]

- Åkerström T, Maharjan R, Sven Willenberg H, Cupisti K, Ip J, Moser A, Stålborg P, Robinson B, Alexander Iwen K, Dralle H, et al. (2016). Activating mutations in CTNNB1 in aldosterone producing adenomas. *Sci. Rep* 6, 19546. [PubMed: 26815163]
- Assié G, Letouzé E, Fassnacht M, Jouinot A, Luscap W, Barreau O, Omeiri H, Rodriguez S, Perlemoine K, René-Corail F, et al. (2014). Integrated genomic characterization of adrenocortical carcinoma. *Nat. Genet* 46, 607–612. [PubMed: 24747642]
- Barker N, Ridgway RA, van Es JH, van de Wetering M, Begthel H, van den Born M, Danenberg E, Clarke AR, Sansom OJ, and Clevers H (2009). Crypt stem cells as the cells-of-origin of intestinal cancer. *Nature* 457, 608–611. [PubMed: 19092804]
- Basham KJ, Rodriguez S, Turcu AF, Lerario AM, Logan CY, Rysztak MR, Gomez-Sanchez CE, Breault DT, Koo B-K, Clevers H, et al. (2019). A ZNRF3-dependent Wnt/ β -catenin signaling gradient is required for adrenal homeostasis. *Genes Dev* 33, 209–220. [PubMed: 30692207]
- Berthon A, Sahut-Barnola I, Lambert-Langlais S, de Joussineau C, Damon-Soubeyrand C, Louiset E, Taketo MM, Tissier F, Bertherat J, Lefrançois-Martinez A-M, et al. (2010). Constitutive beta-catenin activation induces adrenal hyperplasia and promotes adrenal cancer development. *Hum. Mol. Genet* 19, 1561–1576. [PubMed: 20106872]
- Berthon A, Drelon C, Ragazzon B, Boulkroun S, Tissier F, Amar L, Samson-Couterie B, Zennaro M-C, Plouin P-F, Skah S, et al. (2014). WNT/ β -catenin signalling is activated in aldosterone-producing adenomas and controls aldosterone production. *Hum. Mol. Genet* 23, 889–905. [PubMed: 24087794]
- Bielohuby M, Herbach N, Wanke R, Maser-Gluth C, Beuschlein F, Wolf E, and Hoeflich A (2007). Growth analysis of the mouse adrenal gland from weaning to adulthood: time- and gender-dependent alterations of cell size and number in the cortical compartment. *Am. J. Physiol. Endocrinol. Metab* 293, E139–E146. [PubMed: 17374700]
- Chang S-P, Morrison HD, Nilsson F, Kenyon CJ, West JD, and Morley SD (2013). Cell proliferation, movement and differentiation during maintenance of the adult mouse adrenal cortex. *PLoS ONE* 8, e81865. [PubMed: 24324726]
- Côté M, Payet MD, Dufour MN, Guillon G, and Gallo-Payet N (1997). Association of the G protein alpha(q)/alpha11-subunit with cytoskeleton in adrenal glomerulosa cells: role in receptor-effector coupling. *Endocrinology* 138, 3299–3307. [PubMed: 9231781]
- Crona J, and Beuschlein F (2019). Adrenocortical carcinoma - towards genomics guided clinical care. *Nat. Rev. Endocrinol* 15, 548–560. [PubMed: 31147626]
- Crowley SD, Gurley SB, Herrera MJ, Ruiz P, Griffiths R, Kumar AP, Kim H-S, Smithies O, Le TH, and Coffman TM (2006). Angiotensin II causes hypertension and cardiac hypertrophy through its receptors in the kidney. *Proc. Natl. Acad. Sci. USA* 103, 17985–17990. [PubMed: 17090678]
- DeSouza R-M, Jones BRT, Lowis SP, and Kurian KM (2014). Pediatric medulloblastoma - update on molecular classification driving targeted therapies. *Front. Oncol* 4, 176. [PubMed: 25101241]
- Drelon C, Berthon A, Sahut-Barnola I, Mathieu M, Dumontet T, Rodriguez S, Batisse-Lignier M, Tabbal H, Tauveron I, Lefrançois-Martinez A-M, et al. (2016). PKA inhibits WNT signalling in adrenal cortex zonation and prevents malignant tumour development. *Nat. Commun* 7, 12751. [PubMed: 27624192]
- Durand J, Lampron A, Mazzucco TL, Chapman A, and Bourdeau I (2011). Characterization of differential gene expression in adrenocortical tumors harboring β -catenin (CTNNB1) mutations. *J. Clin. Endocrinol. Metab* 96, E1206–E1211. [PubMed: 21565795]
- Dumontet T, Sahut-Barnola I, Septier A, Montanier N, Plotton I, Roucher-Boulez F, Ducros V, Lefrançois-Martinez A-M, Pointud J-C, Zubair M, et al. (2018). PKA signaling drives reticularis differentiation and sexually dimorphic adrenal cortex renewal. *JCI Insight* 3, 3.
- El Wakil A, Mari B, Barhanin J, and Lalli E (2013). Genomic analysis of sexual dimorphism of gene expression in the mouse adrenal gland. *Horm. Metab. Res* 45, 870–873. [PubMed: 23921913]
- Freedman BD, Kempna PB, Carlone DL, Shah M, Guagliardo NA, Barrett PQ, Gomez-Sanchez CE, Majzoub JA, and Breault DT (2013). Adrenocortical zonation results from lineage conversion of differentiated zona glomerulosa cells. *Dev. Cell* 26, 666–673. [PubMed: 24035414]
- Goldstein B, Takeshita H, Mizumoto K, and Sawa H (2006). Wnt signals can function as positional cues in establishing cell polarity. *Dev. Cell* 10, 391–396. [PubMed: 16516841]

- Grabek A, Dolfi B, Klein B, Jian-Motamedi F, Chaboissier M-C, and Schedl A (2019). The Adult Adrenal Cortex Undergoes Rapid Tissue Renewal in a Sex-Specific Manner. *Cell Stem Cell* 25, 290–296. [PubMed: 31104943]
- Harada N, Tamai Y, Ishikawa T, Sauer B, Takaku K, Oshima M, and Taketo MM (1999). Intestinal polyposis in mice with a dominant stable mutation of the beta-catenin gene. *EMBO J* 18, 5931–5942. [PubMed: 10545105]
- Heikkilä M, Peltoketo H, Leppälüoto J, Ilves M, Vuolteenaho O, and Vainio S (2002). Wnt-4 deficiency alters mouse adrenal cortex function, reducing aldosterone production. *Endocrinology* 143, 4358–4365. [PubMed: 12399432]
- Huang Y-L, and Niehrs C (2014). Polarized Wnt signaling regulates ectodermal cell fate in *Xenopus*. *Dev. Cell* 29, 250–257. [PubMed: 24780739]
- Jho EH, Zhang T, Domon C, Joo C-K, Freund J-N, and Costantini F (2002). Wnt/beta-catenin/Tcf signaling induces the transcription of *Axin2*, a negative regulator of the signaling pathway. *Mol. Cell. Biol* 22, 1172–1183. [PubMed: 11809808]
- Kim AC, Reuter AL, Zubair M, Else T, Serecky K, Bingham NC, Lavery GG, Parker KL, and Hammer GD (2008). Targeted disruption of beta-catenin in Sf1-expressing cells impairs development and maintenance of the adrenal cortex. *Development* 135, 2593–2602. [PubMed: 18599507]
- Kitajima K, Oki S, Ohkawa Y, Sumi T, and Meno C (2013). Wnt signaling regulates left-right axis formation in the node of mouse embryos. *Dev. Biol* 380, 222–232. [PubMed: 23707899]
- Koo B-K, Spit M, Jordens I, Low TY, Stange DE, van de Wetering M, van Es JH, Mohammed S, Heck AJR, Maurice MM, and Clevers H (2012). Tumour suppressor RNF43 is a stem-cell E3 ligase that induces endocytosis of Wnt receptors. *Nature* 488, 665–669. [PubMed: 22895187]
- Lippert J, Appenzeller S, Liang R, Sbiera S, Kircher S, Altieri B, Nanda I, Weigand I, Gehrig A, Steinhauer S, et al. (2018). Targeted Molecular Analysis in Adrenocortical Carcinomas: A Strategy Toward Improved Personalized Prognostication. *J. Clin. Endocrinol. Metab* 103, 4511–4523. [PubMed: 30113656]
- Loh KM, van Amerongen R, and Nusse R (2016). Generating Cellular Diversity and Spatial Form: Wnt Signaling and the Evolution of Multicellular Animals. *Dev. Cell* 38, 643–655. [PubMed: 27676437]
- MacFarland RT, Zelus BD, and Beavo JA (1991). High concentrations of a cGMP-stimulated phosphodiesterase mediate ANP-induced decreases in cAMP and steroidogenesis in adrenal glomerulosa cells. *J. Biol. Chem* 266, 136–142. [PubMed: 1845962]
- Mathieu M, Drelon C, Rodriguez S, Tabbal H, Septier A, Damon-Soubeyrand C, Dumontet T, Berthon A, Sahut-Barnola I, Djari C, et al. (2018). Steroidogenic differentiation and PKA signaling are programmed by histone methyltransferase EZH2 in the adrenal cortex. *Proc. Natl. Acad. Sci. USA* 115, E12265–E12274. [PubMed: 30541888]
- McEwan PE, Vinson GP, and Kenyon CJ (1999). Control of adrenal cell proliferation by AT1 receptors in response to angiotensin II and low-sodium diet. *Am. J. Physiol* 276, E303–E309. [PubMed: 9950790]
- Muñoz-Durango N, Fuentes CA, Castillo AE, González-Gómez LM, Vecchiola A, Fardella CE, and Kalergis AM (2016). Role of the Renin-Angiotensin-Aldosterone System beyond Blood Pressure Regulation: Molecular and Cellular Mechanisms Involved in End-Organ Damage during Arterial Hypertension. *Int. J. Mol. Sci* 17, E797. [PubMed: 27347925]
- Muzumdar MD, Tasic B, Miyamichi K, Li L, and Luo L (2007). A global double-fluorescent Cre reporter mouse. *Genesis* 45, 593–605. [PubMed: 17868096]
- Nishimoto K, Harris RBS, Rainey WE, and Seki T (2014). Sodium deficiency regulates rat adrenal zona glomerulosa gene expression. *Endocrinology* 155, 1363–1372. [PubMed: 24422541]
- Nusse R, and Clevers H (2017). Wnt/ β -Catenin Signaling, Disease, and Emerging Therapeutic Modalities. *Cell* 169, 985–999. [PubMed: 28575679]
- Pignatti E, Leng S, Carlone DL, and Breault DT (2017). Regulation of zonation and homeostasis in the adrenal cortex. *Mol. Cell. Endocrinol* 441, 146–155. [PubMed: 27619404]
- Polakis P (2012). Wnt signaling in cancer. *Cold Spring Harb. Perspect. Biol* 4, a008052. [PubMed: 22438566]

- Ragazzon B, Libé R, Gaujoux S, Assié G, Fratticci A, Launay P, Clauser E, Bertagna X, Tissier F, Reynié A, and Bertherat J (2010). Transcriptome analysis reveals that p53 and beta-catenin alterations occur in a group of aggressive adrenocortical cancers. *Cancer Res* 70, 8276–8281. [PubMed: 20959480]
- Romagnolo B, Berrebi D, Saadi-Keddoucci S, Porteu A, Pichard AL, Peuchmaur M, Vandewalle A, Kahn A, and Perret C (1999). Intestinal dysplasia and adenoma in transgenic mice after overexpression of an activated beta-catenin. *Cancer Res* 59, 3875–3879. [PubMed: 10463573]
- Romero DG, Yanes LL, de Rodriguez AF, Plonczynski MW, Welsh BL, Reckelhoff JF, Gomez-Sanchez EP, and Gomez-Sanchez CE (2007). Disabled-2 is expressed in adrenal zona glomerulosa and is involved in aldosterone secretion. *Endocrinology* 148, 2644–2652. [PubMed: 17303656]
- Sansom OJ, Meniel VS, Muncan V, Pheesse TJ, Wilkins JA, Reed KR, Vass JK, Athineos D, Clevers H, and Clarke AR (2007). Myc deletion rescues Apc deficiency in the small intestine. *Nature* 446, 676–679. [PubMed: 17377531]
- Sastre-Perona A, and Santisteban P (2012). Role of the wnt pathway in thyroid cancer. *Front. Endocrinol. (Lausanne)* 3, 31. [PubMed: 22645520]
- Schindelin J, Arganda-Carreras I, Frise E, Kaynig V, Longair M, Pietzsch T, Preibisch S, Rueden C, Saalfeld S, Schmid B, et al. (2012). Fiji: an open-source platform for biological-image analysis. *Nat. Methods* 9, 676–682. [PubMed: 22743772]
- Schneider J, Arraf AA, Grinstein M, Yelin R, and Schultheiss TM (2015). Wnt signaling orients the proximal-distal axis of chick kidney nephrons. *Development* 142, 2686–2695. [PubMed: 26116665]
- Sequine S, Shibata T, Kokubu A, Morishita Y, Noguchi M, Nakanishi Y, Sakamoto M, and Hirohashi S (2002). Craniopharyngiomas of adamantinomatous type harbor beta-catenin gene mutations. *Am. J. Pathol* 161, 1997–2001. [PubMed: 12466115]
- Spinedi E, Suescun MO, Hadid R, Daneva T, and Gaillard RC (1992). Effects of gonadectomy and sex hormone therapy on the endotoxin-stimulated hypothalamo-pituitary-adrenal axis: evidence for a neuroendocrine-immunological sexual dimorphism. *Endocrinology* 131, 2430–2436. [PubMed: 1330501]
- Stephenson DT, Coskran TM, Wilhelms MB, Adamowicz WO, O'Donnell MM, Muravnick KB, Menniti FS, Kleiman RJ, and Morton D (2009). Immunohistochemical localization of phosphodiesterase 2A in multiple mammalian species. *J. Histochem. Cytochem* 57, 933–949. [PubMed: 19506089]
- Teo J-L, Ma H, Nguyen C, Lam C, and Kahn M (2005). Specific inhibition of CBP/beta-catenin interaction rescues defects in neuronal differentiation caused by a presenilin-1 mutation. *Proc. Natl. Acad. Sci. USA* 102, 12171–12176. [PubMed: 16093313]
- Tissier F, Cavard C, Groussin L, Perlempoine K, Fumey G, Hagneré A-M, René-Corail F, Jullian E, Gicquel C, Bertagna X, et al. (2005). Mutations of beta-catenin in adrenocortical tumors: activation of the Wnt signaling pathway is a frequent event in both benign and malignant adrenocortical tumors. *Cancer Res* 65, 7622–7627. [PubMed: 16140927]
- Vidal V, Sacco S, Rocha AS, da Silva F, Panzolini C, Dumontet T, Doan TMP, Shan J, Rak-Raszewska A, Bird T, et al. (2016). The adrenal capsule is a signaling center controlling cell renewal and zonation through Rspo3. *Genes Dev* 30, 1389–1394. [PubMed: 27313319]
- Walczak EM, and Hammer GD (2015). Regulation of the adrenocortical stem cell niche: implications for disease. *Nat. Rev. Endocrinol* 11, 14–28. [PubMed: 25287283]
- Walczak EM, Kuick R, Finco I, Bohin N, Hrycaj SM, Wellik DM, and Hammer GD (2014). Wnt signaling inhibits adrenal steroidogenesis by cell-autonomous and non-cell-autonomous mechanisms. *Mol. Endocrinol* 28, 1471–1486. [PubMed: 25029241]
- Wang JJ, Peng KY, Wu VC, Tseng FY, and Wu KD (2017). CTNNB1 Mutation in Aldosterone Producing Adenoma. *Endocrinol. Metab. (Seoul)* 32, 332–338. [PubMed: 28956362]
- Wu V-C, Wang S-M, Chueh SJ, Yang S-Y, Huang K-H, Lin Y-H, Wang J-J, Connolly R, Hu Y-H, Gomez-Sanchez CE, et al. (2017). The prevalence of CTNNB1 mutations in primary aldosteronism and consequences for clinical outcomes. *Sci. Rep* 7, 39121. [PubMed: 28102204]

- Zajicek G, Ariel I, and Arber N (1986). The streaming adrenal cortex: direct evidence of centripetal migration of adrenocytes by estimation of cell turnover rate. *J. Endocrinol* 111, 477–482. [PubMed: 3805971]
- Zhan T, Rindtorff N, and Boutros M (2017). Wnt signaling in cancer. *Oncogene* 36, 1461–1473. [PubMed: 27617575]
- Zheng S, Cherniack AD, Dewal N, Moffitt RA, Danilova L, Murray BA, Lerario AM, Else T, Knijnenburg TA, Ciriello G, et al.; Cancer Genome Atlas Research Network (2016). Comprehensive Pan-Genomic Characterization of Adrenocortical Carcinoma. *Cancer Cell* 29, 723–736. [PubMed: 27165744]

Author Manuscript

Author Manuscript

Author Manuscript

Author Manuscript

HIGHLIGHTS

- β -catenin activation drives adrenal hyperplasia by blocking cellular differentiation
- Upregulation of Pde2a, an inhibitor of cAMP/PKA, is a potential mechanism for the block
- Hyperplasia is exacerbated by trophic factor stimulation leading to organomegaly

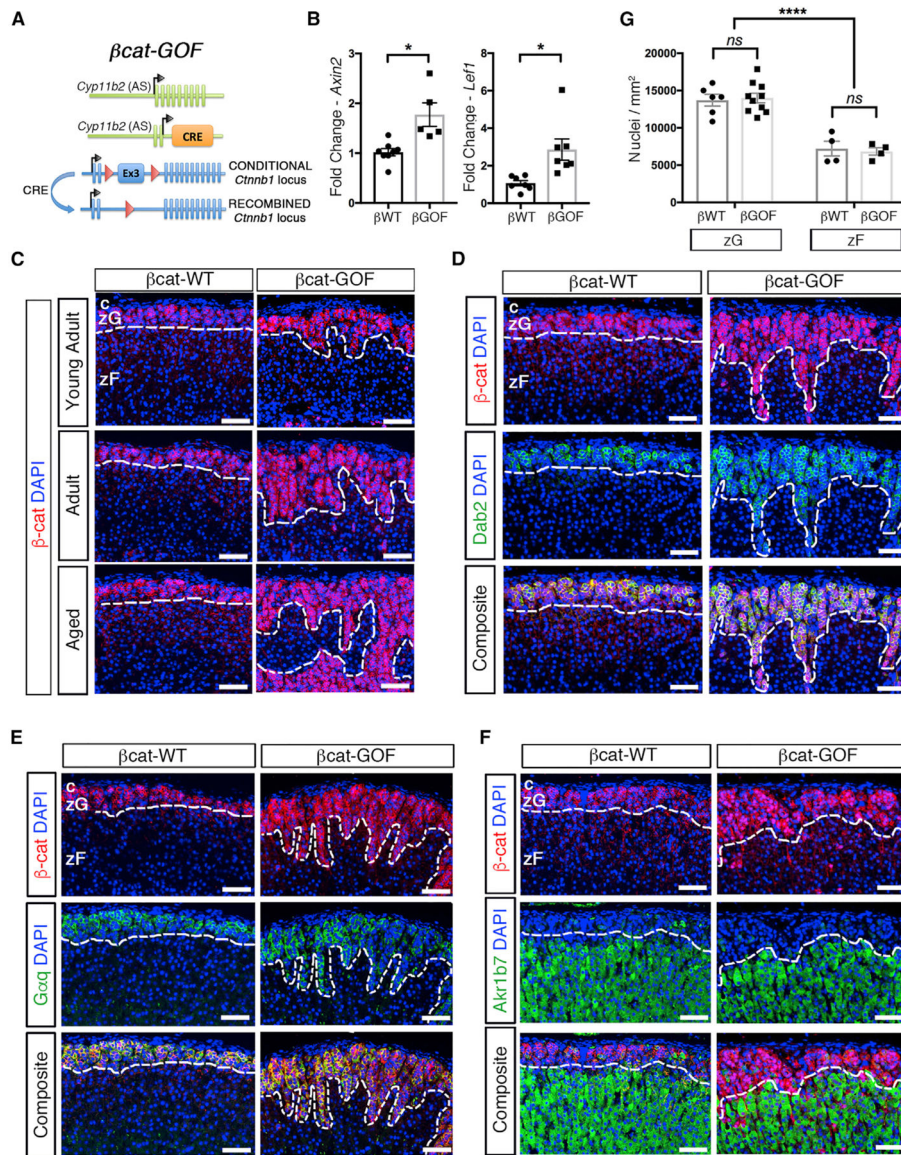


Figure 1. Stabilization of β -Catenin in zG Cells Results in Expansion of the zG
 (A) Schematic representation of the alleles comprising β cat-GOF (bGOF) mice. Cre recombinase is expressed under the control of the aldosterone synthase (AS) promoter and drives excision of the third LoxP-flanked exon of *Ctnnb1*, encoding β -catenin, leading to stabilization in AS-expressing zG cells. β cat-WT (bWT) control mice have two copies of the wild-type *Ctnnb1* allele.
 (B) Quantitative real-time PCR for *Axin2* ($n = 7$ β cat-WT and 5 β cat-GOF mice) and *Lef1* ($n = 7$ β cat-WT and 6 β cat-GOF mice).
 (C) Representative adrenal sections stained for β -catenin (β -cat, red) ($n = 5$ β cat-WT and 10 β cat-GOF mice).
 (D) Representative adrenal sections co-stained for β -catenin (β -cat, red) and Dab2 (green) ($n = 3$ β cat-WT and 4 β cat-GOF mice).
 (E) Representative adrenal sections co-stained for β -catenin (β -cat, red) and Gata3 (green) ($n = 3$ β cat-WT and 4 β cat-GOF mice).
 (F) Representative adrenal sections co-stained for β -catenin (β -cat, red) and Akrlb7 (green) ($n = 3$ β cat-WT and 4 β cat-GOF mice).
 (G) Quantification of nuclei per mm² in zG and zF regions. **** indicates $p < 0.0001$, ns indicates not significant.

(E) Representative adrenal sections co-stained for β -catenin (β -cat, red) and G α q (green) ($n = 7$ β cat-WT and 9 β cat-GOF mice).

(F) Representative adrenal sections co-stained for β -catenin (β -cat, red) and Akr1b7 (green) ($n = 3$ mice for each genotype).

(G) Analysis of cellular density using quantification of DAPI-stained nuclei normalized per unit area (dots represent single measurements; n from left to right = 6, 10, 4, 4). All sections were counterstained with nuclear DAPI (blue) and were from adult mice unless otherwise stated. The dotted lines define the border between β -catenin-positive and -negative regions. c, capsule.

zG, zona Glomerulosa. zF, zona Fasciculata. Scale bars: 50 μ m. *ns*, not significant. * $p < 0.05$; **** $p < 0.0001$. Data are represented as mean \pm SEM.

See also Figure S1.

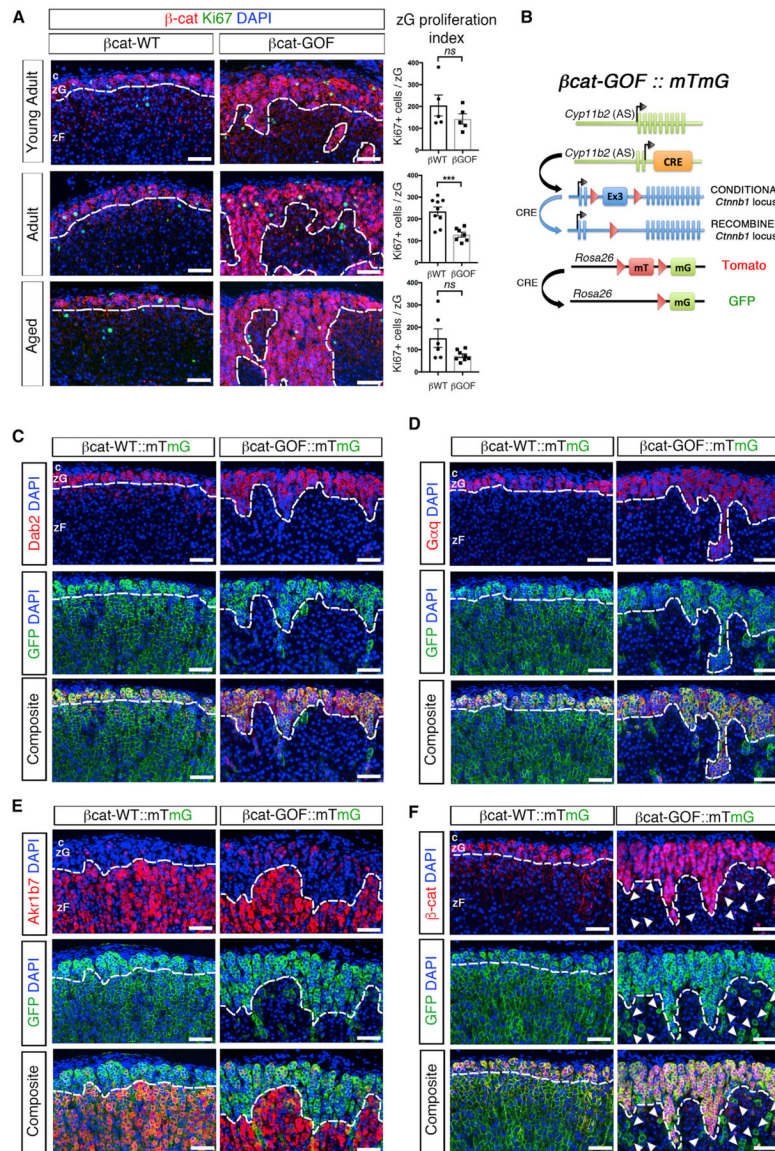


Figure 2. Stabilization of β -Catenin in zG Cells Blocks zG-to-zF cell Transdifferentiation

(A) Left: representative adrenal sections co-stained for β -catenin (β -cat, red) and Ki67 (green). Right: quantification of the Ki67-positive cells normalized for the β -catenin-positive zG domain (zG proliferation index) (from left to right, top to bottom, n = 5, 5, 9, 7, 6, 8 mice).

(B) Schematic representation of the alleles comprising β cat-GOF::mTmG mice. β cat-WT::mTmG control mice have two copies of the wild-type *Ctnnb1* allele.

(C) Representative adrenal sections co-stained for Dab2 (red) and GFP (green) (n = 9 mice for each genotype).

(D) Representative adrenal sections co-stained for G α q (red) and GFP (green) (n = 9 mice for each genotype).

(E) Representative adrenal sections co-stained Akr1b7 (red) and GFP (green) (n = 3 mice for each genotype).

(F) Representative adrenal sections co-stained for β -catenin (β -cat, red) and GFP (green) ($n = 5$ mice for each genotype). All sections were counterstained with nuclear DAPI (blue) and were from adult mice. Arrowheads point at GFP-positive and β -catenin-negative zF cells. All dotted lines define the border between positive and negative regions for β -catenin, Dab2, G α q, or Akr1b7, as indicated.

c, capsule. zG, zona Glomerulosa. zF, zona Fasciculata. Scale bars: 50 μ m. *ns*, not significant; *** $p < 0.001$. Data are represented as mean \pm SEM.

See also Figure S2.

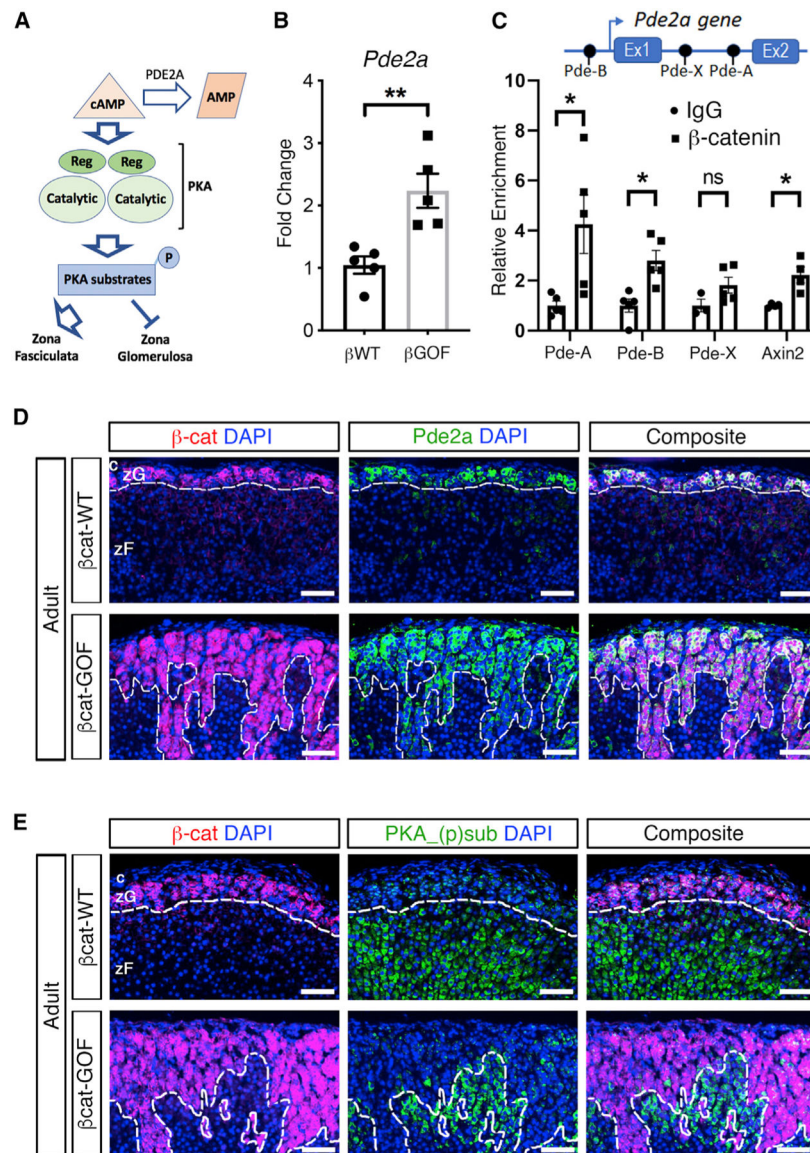


Figure 3. Stabilization of β -Catenin in zG Cells Results in Upregulation of Pde2a

(A) Schematic representation of the effects of the cAMP/PKA signaling pathway on zG and zF. Pde2a catalyzes the hydrolysis of cAMP to AMP.

(B) Quantitative real-time PCR for *Pde2a* ($n = 5$ mice for each genotype).

(C) Chromatin immunoprecipitation of three consensus TCF/LEF sequences within the *Pde2a* gene, named Pde-A, Pde-B and Pde-X, located at +19,762 bp (within the first intron), -8,545 bp (within the distal promoter), and +873 bp (within the first intron) with respect to the transcriptional start site (arrow). The well-characterized consensus TCF/LEF site within *Axin2*, located at +1,926 bp, was used as positive control (Jho et al., 2002). Fold change relative to IgG. Statistical analysis was performed using Welch's t test ($n = 4-5$).

(D) Representative adrenal sections co-stained for β -catenin (β -cat, red) and Pde2a (green) ($n = 3$ mice for each genotype).

(E) Representative adrenal sections co-stained for β -catenin (β -cat, red) and phosphorylated substrates of PKA (PKA_(p)sub, green), (n = 3 mice for each genotype). All sections were counterstained with nuclear DAPI (blue) and were from adult mice. The dotted lines define the border between positive and negative regions for β -catenin. c, capsule. zG, zona Glomerulosa; zF, zona Fasciculata; p, phosphorylation; Ex, exon(s). Scale bars: 50 μ m. *ns*, not significant; **p* < 0.05, ***p* < 0.01. Data are represented as mean \pm SEM.

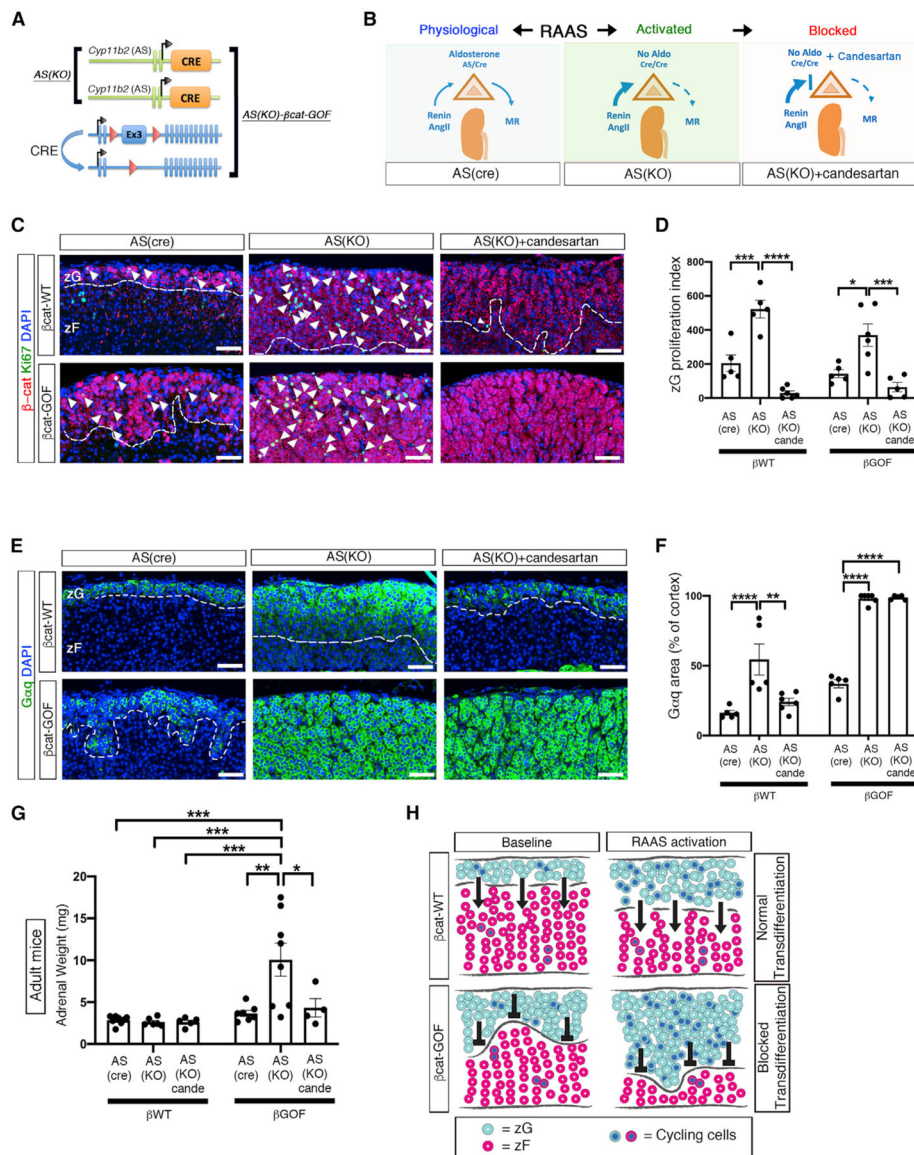


Figure 4. Activation of RAAS Leads to Marked Adrenal Hyperplasia

(A) Schematic representation of the alleles comprising AS(KO) and AS(KO)- β cat-GOF mice. The presence of two AS-Cre alleles results in RAAS activation.

(B) Left: schematic representation of RAAS under physiological conditions. Center: activation of RAAS in AS(KO) mice. Right: RAAS activity is blocked by the AngII receptor antagonist Candesartan.

(C) Representative adrenal sections co-stained for β -catenin (β -cat, red) and Ki67 (green). Arrowheads mark co-positive cells.

(D) Quantification of the Ki67-positive cells from (C) normalized for the β -catenin-positive domain (zG proliferation index).

(E) Representative adrenal sections stained for G α q (green).

(F) Quantification of G α q-positive area from (E) normalized for cortical area.

(C and D) From left to right and top to bottom: n = 5, 5, 6, 5, 6, and 5 mice.

(E and F) From left to right: n = 5, 5, 6, 5, 6, and 5 mice.

(G) Weight of adrenal glands from adult mice (from left to right, n = 8, 6, 5, 7, 8, and 4 mice).

(H) Schematic representation of the effect of RAAS activation on β -catenin mice. Light blue circles represent zG cells. Red circles represent zF cells. Blue nuclei indicate proliferating cells. Arrows (\rightarrow) indicate the ongoing process of zG-to-zF cell transdifferentiation, which allows zG cells to migrate into the zF. Transdifferentiation is blocked in β cat-GOF adrenals, as indicated by the symbol (\perp). zG proliferation index (total number of Ki67-positive cells normalized by zG area) is decreased or unaltered in zG of β cat-GOF compared to controls and increased in β cat-GOF exposed to activated RAAS. All stained sections were counterstained with nuclear DAPI (blue) and were obtained from young adult mice. The dotted lines define the border between β -catenin/ $G\alpha_q$ -positive and -negative regions. zG, zona Glomerulosa; zF, zona Fasciculata; MR, mineralocorticoid receptors; Aldo, aldosterone; AngII, Angiotensin II; cande, Candesartan. Scale bars: 50 μ m. *p < 0.05; **p < 0.01; ***p < 0.001; ****p < 0.0001. Data are represented as mean \pm SEM.

KEY RESOURCES TABLE

REAGENT or RESOURCE	SOURCE	IDENTIFIER
Antibodies		
Mouse monoclonal anti- β -catenin	BD Biosciences	Cat# 610153; RRID: AB_397554
Rabbit polyclonal anti- β -catenin	Abcam	Cat# ab16051; RRID: AB_443301
Chicken polyclonal anti-GFP	Aves Labs	Cat# GFP-1020; RRID: AB_10000240
Rabbit monoclonal anti-Caspase-3, Active Form	BD Biosciences	Cat# 559565; RRID:AB_397274
Mouse monoclonal anti p-96/Dab2	BD Biosciences	Cat# 610464; RRID:AB_397837
Rabbit polyclonal anti-Akr1b7	Dr Pierre Val and Dr Antoine Martinez; (Aigueperse et al., 1999)	N/A
Rabbit polyclonal anti-G α q	Abcam	Cat# ab75825; RRID:AB_1925009
Rabbit polyclonal anti-AS	Dr. Celso E. Gomez-Sanchez; (Freedman et al., 2013)	N/A
Rabbit monoclonal anti-Ki67	Lab Vision	Cat# RM-9106; RRID:AB_2335745
Rabbit monoclonal anti-Lef1	Abcam	Cat# ab137872
Rabbit polyclonal anti-Phospho-(Ser/Thr) PKA Substrate	Cell Signaling Technology	Cat# 9621; RRID:AB_330304
Rabbit monoclonal anti- β -catenin(ex3)	Abcam	Cat# ab32572; RRID:AB_725966
Rabbit polyclonal anti-PDE2A	Proteintech	Cat# 55306-1-AP; RRID:AB_11182279
Donkey anti-Rabbit IgG (H+L) Highly Cross-Adsorbed Secondary Antibody, Alexa Fluor 647	Molecular Probes	Cat# A-31573; RRID:AB_2536183
Mouse IgG (H+L) Highly Cross-Adsorbed Secondary Antibody, Alexa Fluor 594	Thermo Fisher Scientific	Cat# A32742; RRID:AB_2762825
Goat anti-Chicken IgY (H+L) Cross-Adsorbed Secondary Antibody, Alexa Fluor Plus 488	Thermo Fisher Scientific	Cat# A32931; RRID:AB_2762843
Rabbit polyclonal anti- β -catenin	Cell Signaling Technology	Cat# 9581; RRID:AB_490891
Rabbit polyclonal anti-Histone H3	Abcam	Cat# ab1791, RRID:AB_302613
Chemicals, Peptides, and Recombinant Proteins		
Angiotensinogen 1-14 renin substrate porcine	Sigma Aldrich	Cat# SCP0021-1MG
Critical Commercial Assays		
Direct-zol RNA Miniprep	Zymo Research	Cat# R2051
High-Capacity cDNA Reverse Transcription Kit	Thermo Fisher Scientific	Cat# 4368814
TaqMan Universal PCR Master Mix	Thermo Fisher Scientific	Cat# 4364338
Click-iT Plus TUNEL Assay for <i>In Situ</i> Apoptosis Detection, Alexa Fluor 488 dye	Thermo Fisher Scientific	Cat# C10617
Aldosterone RIA (CT)	Tecan	Cat# MG13051
Angiotensin I (PRA) RIA (CT)	Tecan	Cat# 30120823
High-Sensitivity ChIP Kit	Abcam	Cat# ab185913
Power SYBR Green PCR Master Mix	Thermo Fisher Scientific	Cat# 4367659
Experimental Models: Organisms/Strains		

REAGENT or RESOURCE	SOURCE	IDENTIFIER
Mouse: AS-Cre: 129-Cyp11b2 ^{tm1.1(cre)Br/t+}	Our lab(Freedman et al., 2013)	N/A
Mouse: Ctnnb1 ^{flox(ex3)/+} ; 129-Ctnnb1 ^{tm1Mmt/+}	Harada et al., 1999	MGI:1858008
Mouse: mTmG: 129-Gt(ROSA) ^{26Sortm4(ACTB-tdTomato,-EGFP)Luo/J/+}	The Jackson Laboratory	JAX:007576
Oligonucleotides		
See Table S1 for all oligos and primers.		N/A
Software and Algorithms		
Prism v8.3.0	Graphpad	https://www.graphpad.com/scientific-software/prism/
Fiji	Schindelin et al., 2012	https://fiji.sc/
LIS-Elements Nikon	Nikon	https://www.microscope.healthcare.nikon.com/products/software/nis-elements